RSC Advances

PAPER

View Article Online
View Journal | View Issue

Cite this: *RSC Adv.*, 2017, **7**, 275

High pressure studies of Eu^{2+} and Mn^{2+} doped $NaScSi_2O_6$ clinopyroxenes†

J. Barzowska,[a] Zhiguo Xia,[b] D. Jankowski,[c] D. Włodarczyk,[c] K. Szczodrowski,[a] Chong-Geng Ma,[d] M. G. Brik,[def] Ya. Zhydachevskii[c] and A. Suchocki*[cdg]

Received 7th October 2016
Accepted 27th October 2016

DOI: 10.1039/c6ra24854c

www.rsc.org/advances

High pressure luminescence studies of $NaScSi_2O_6$ clinopyroxene (jervisite) doped with Eu^{2+} and Mn^{2+} are reported. The efficiency of the energy transfer between Eu^{2+} and Mn^{2+} is examined. It is shown that the efficiency of the energy transfer process is weakly dependent on pressure, although a small increase of the probability of nonradiative energy transfer with increase of pressure is observed. In contrast to that the energy transfer efficiency at ambient pressure is independent of temperature between 10 K and 400 K. The Raman spectra under pressure shows fingerprints of the reversible phase transitions at pressures of about 100–120 kbar at room temperature. The occurrence of the phase transition drastically reduces the efficiency of energy transfer, which is restored at higher pressures. The Mn^{2+} luminescence is quenched at about 200 kbar due to the crossing between the $^4T_{1g}$ and $^2T_{2g}$ excited states occurring at this pressure. The $^2T_{2g}$ state becomes the first excited level at this pressure and due to much stronger coupling with the host the Mn^{2+} luminescence is quenched. This is the first observation of such behaviour for Mn^{2+} ions. Pressure dependence of CIE color coordinates is established for this phosphor.

I. Introduction

Recent development of white-light emitting diodes (WLED) and attempts to obtain the most efficient phosphors for diodes with controlled color-rendering index and high correlated color temperature have triggered a great number of studies of various materials, sometimes quite exotic, although existing in nature, or intentionally designed for these purposes. One such material is Na–clinopyroxene with general chemical formula $NaMe^{3+}Si_2O_6$. This material has a monoclinic crystallographic structure with space group $C2/c$ at ambient pressure.[1] Clinopyroxenes (monoclinic pyroxenes) are components of various minerals, as for example: augite, diopside, pigeonite, hedenbergite, aegirine, jadeite ($Na(Al,Fe^{3+})Si_2O_6$) and omphacite. They are most common in basic and ultrabasic igneous rocks such as basalt, gabbro, peridotite and pyroxenite. Fe-rich clinopyroxenes can occur within granites, diorites and syenites. Alkali-rich clinopyroxenes are particularly abundant in alkaline igneous rocks such as phonolites, basanites, nephelinites *etc.*[2,3] and they are important components of upper Earth mantle,[4,5] at least partially determining its seismic properties. Recent studies of $NaScSi_2O_6$:Eu^{2+} and Mn^{2+} clinopyroxene (this type of clinopyroxene is called jervisite)[6] and similar compounds showed that they might be useful as phosphors for WLED, being stable over a wide range of pressures and temperatures, exhibiting useful emission properties with possibility of tuning photoluminescence by using solid solutions between various compounds in clinopyroxene family.[6,7]

Me^{3+} ions are located in octahedral coordination in clinopyroxene host. It has been established with use of XRD data that Eu^{2+} ions substitute Na ions in distorted cubic antiprism polyhedrons and Mn^{2+} are in octahedral coordination replacing Sc ions.[1] The site occupancy is related to ionic radii of dopant and host ions, which actually is the most important factor establishing preference in choosing the sites for dopant location.

Previous photoluminescence studies showed that samples of $NaScSi_2O_6$ doped only with Eu^{2+} exhibit typical green emission. By codoping with Mn^{2+} due to the energy transfer from Eu^{2+} ions to Mn^{2+} the color of emission can be changed from green to yellow due to existence of additional luminescence band with maximum at about 660 nm. This bad is associated with typical Mn^{2+} luminescence due to the $^4T_1 \rightarrow {}^6A_1$ intraconfigurational transitions within electronic states of the Mn^{2+} ions. The

[a]*Institute of Experimental Physics, Gdańsk University, ul. Wita Stwosza 57, 80-952 Gdańsk, Poland*

[b]*The Beijing Municipal Key Laboratory of New Energy Materials and Technologies, School of Materials Sciences and Engineering, University of Science and Technology Beijing, Beijing 100083, China*

[c]*Institute of Physics, Polish Academy of Sciences, Al. Lotników 32/46, 02-668 Warsaw, Poland. E-mail: suchy@ifpan.edu.pl*

[d]*College of Mathematics and Physics, Chongqing University of Posts and Telecommunications, Chongqing 400065, PR China*

[e]*Institute of Physics, University of Tartu, W. Ostwald Str. 1, Tartu 50411, Estonia*

[f]*Institute of Physics, Jan Dlugosz University, Al. Armii Krajowej 13/15, Czestochowa PL-42200, Poland*

[g]*Institute of Physics, Kazimierz Wielki University, Weyssenhoffa 11, 85-072 Bydgoszcz, Poland*

† Electronic supplementary information (ESI) available. See DOI: 10.1039/c6ra24854c

emission color on the CIE chromaticity diagram depends on the concentration of Mn^{2+} codopant.[1]

In order to check further possibility of controlling the luminescence color in these types of compounds we decided to study the effect of hydrostatic pressure on the luminescence properties of clinopyroxenes doped with both Eu^{2+} and Mn^{2+} ions. Application of high pressures can effectively change the inter-atomic distances in the solid state materials (depending on pressure and bulk modulus of the material studied – even up to a few tens of %). Therefore the strength of the crystal field experienced by central ions can be effectively changed. If the position of the luminescence is strongly dependent on strength of the crystal field, which is the case of the Eu^{2+} 5d → 4f transitions[8,9] or intraconfigurational Mn^{2+} optical transitions,[10] the color of the emission can be considerably changed by pressure application. This allows for establishing conditions for "chemical pressure" use, *i.e.* by changing the interatomic distances due to the change of the lattice parameters as the result of preparation of solid solutions with various materials having different lattice parameters associated with different ionic radii of host ions. In this way high pressure application, which can be done in precise and controlled way, allows to check and establish conditions for obtaining the desired luminescence properties of the material for practical applications. Important parts of these effects are details of the energy transfer processes and influence of pressure on the observed phenomena. These are the aims of the present publication.

II. Samples and experimental methods

Samples used for the study were prepared by the sol–gel method and had powdered form. The details of preparation procedure can be found in ref. 1. Three types of samples were studied in details: singly doped $NaScSi_2O_6$:Eu(5%), $NaScSi_2O_6$:Mn(5%), and doubly doped $NaScSi_2O_6$:Eu(5%),Mn(15%). The sample with 15% of Mn^{2+} was chosen due to the importance of effect of the energy transfer between the Eu^{2+} and Mn^{2+} ions and associated with this efficient Mn^{2+} emission, but with small, on the other hand, effect of concentration quenching, observed for samples with higher concentration of dopants.[1]

The quality and phase purity of the chosen samples were examined with X-ray diffraction method (XRD) using BRUKER D2PHASER equipment employing Cu K_α radiation and operated at 30 kV and 10 mA. The XRD patterns were collected using scanning step of 0.02° and counting time of 1 s per step. The phase analysis was carried out using DIFFRAC.EVA V4.1 evaluating application from BRUKER.

The results of XRD analysis are in agreement with results previously presented in ref. 1. The samples besides desired phase of $NaScSi_2O_6$ contain also small amount of additional phases. It may be due to the high level of doping with Eu^{2+} and Mn^{2+}. It seems that there is a small amount of hydrated silicas, as well as scandium pyrosilicate ($Sc_2Si_2O_7$), scandium oxide and in the doubly doped (with Eu^{2+} and Mn^{2+}) sample – also Eu_2O_3. There are no impurity phases containing manganese. The amount of various additional phases is difficult to be estimated, although qualitative analysis shows that the phase of clinopyroxene $NaScSi_2O_6$ is strongly dominating. The examples of diffractograms with detailed phase analysis are shown in ESI.†

Excitation spectra at ambient pressure were acquired using Fluorolog 3 (Horiba) spectrofluorimeter. Photoluminescence spectra were measured using Shamrock SR750 D1 grating spectrometer equipped with iDus 420 CCD detector (Andor Technology). The IK5352R-D He–Cd continuous wave laser (Kimmon Koha) was used as an excitation source. For high pressure experiments the samples were placed in a Merrill-Bassett type diamond anvil cell (DAC). Polydimethylsiloxane oil was used as a pressure-transmitting medium, and ruby as pressure gauge.

The experimental setup for luminescence kinetics and time resolved emission spectra consisted of a YAG:Nd laser of PL2143A/SS type and a parametric optical generator PG401/SH. The laser generated 30 ps pulses at 355 nm wavelength with repetition frequency of 10 Hz. The laser pumped PG generator could produce light pulses at wavelengths ranging from 220 nm to 2200 nm. The emission signal was analyzed with the 2501S (BrukerOptics) spectrometer and a Hamamatsu Streak Camera model C4334-01. Luminescence decays were collected by the integration of streak camera images over the wavelength intervals.

For temperature dependent measurements the sample was placed in closed-cycle helium cryostat. The system consisted of water cooled helium compressor model ARS-4HW and expander model DE-204SI (Advanced Research System, Inc.) and Lake-Shore temperature controller Model 336.

The high-pressure Raman spectra at room temperature were taken using MonoVista CRS+ Raman system equipped with 532 nm laser. Powdered samples were placed in the Diacell CryoDAC-LT of Almax easyLab. Argon was used as a pressure transmitting medium and ruby as a pressure gauge.

III. Experimental results

III.1. Ambient pressure studies

The $NaScSi_2O_6$ doped with Eu(5%) and doubly doped with Eu(5%) and Mn(15%) exhibit strong luminescence in the green spectral region related to the Eu^{2+} 5d → 4f transitions (with a peak at 550 nm) and Mn^{2+} $^4T_{1g}$ → $^6A_{1g}$ transitions (with a maximum around 660 nm), if excited in the UV region. Weaker luminescence is observed from only Mn^{2+}-doped sample, due to the forbidden character of the absorption within the 3d shell of the Mn^{2+} ions. Normalized luminescence spectra of $NaScSi_2O_6$:Eu(5%) and $NaScSi_2O_6$:Eu(5%),Mn(15%) taken at room temperature, are presented in Fig. 1.

The peak of the Mn^{2+} band is located in the red region, which means that the Mn^{2+} ions experience quite strong crystal field. Normalized excitation spectra of both samples, monitored at the peaks of their luminescence bands, are presented in Fig. 2a.

The excitation spectra exhibit very good concurrence and they are in agreement with excitation of both dopants through the Eu^{2+} ions. Mn^{2+} ions are mainly excited by the efficient energy transfer from Eu^{2+} ions due to the Forster–Dexter energy

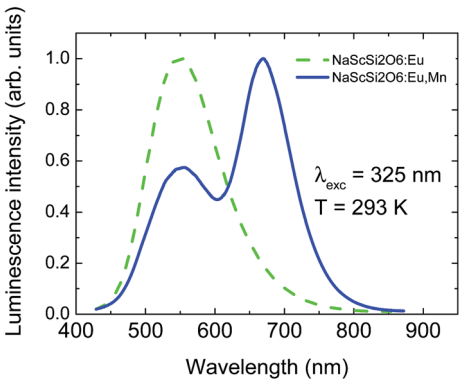

Fig. 1 Normalized luminescence spectra of $NaScSi_2O_6$:Eu(5%) and $NaScSi_2O_6$:Eu(5%),Mn(15%) samples at room temperature under 325 nm excitation.

transfer mechanism, which will be discussed later. No excitation bands associated with the transitions from the ground $^6A_{1g}$ state to the $^4T_{1g}$ and $^4T_{2g}$ states are visible in the excitation spectra of Mn^{2+} ions, in agreement with spin-forbidden character of these transitions. Fig. 2a shows unambiguously that the nonradiative energy transfer mechanism is the most efficient way of excitation of Mn^{2+} ions in this system. Only some traces of the $^4A_{1g}$ + ^4E_g band are visible in the Mn^{2+} excitation spectra around 415 nm. This band is usually one of the strongest in the absorption and PLE spectra of Mn^{2+} ions.

Much weaker Mn^{2+} luminescence is observed in the sample doped only with Mn^{2+}. Its excitation spectra monitored at 530 nm and 650 nm are presented in Fig. 2b. Some traces of the Eu^{2+} dopant can be found in this sample, which gives a very weak green luminescence with a peak at about 530 nm. The bands associated with transitions to the $^4T_{1g}$ and $^4T_{2g}$ states are not detected in the excitation spectrum of Mn^{2+} ions recorded at 650 nm, however some weak bands related to transitions to the ^4E_g + $^4A_{1g}$ states can be observed at the wavelength around 415 nm, as well as some higher energy states of Mn^{2+} at shorter wavelengths. The strong excitation band, with a maximum at about 270 nm is the most likely related to band-gap excitation mechanism of both Mn^{2+} and Eu^{2+} dopants in this compound. It is also visible in the excitation spectra of two other samples, presented in Fig. 2, however on the high-energy side of the very strong band associated with the 4f → 5d excitation of Eu^{2+}. Decrease of the excitation efficiency observed at higher energy side of this band is related to the smaller penetration depth of the excitation light due to the very strong band-to-band absorption of the host. The spectral position of this band implies that the band-gap of jervisite is larger than previously estimated[1] and it is equal to about 4.0 eV (310 nm).

The temperature dependence of the luminescence spectra of the $NaScSi_2O_6$:Eu(5%),Mn(15%) sample are shown in Fig. 3.

The temperature dependent decay kinetics of Eu^{2+} and Mn^{2+} for $NaScSi_2O_6$:Eu(5%),Mn(15%) sample are shown in Fig. 4a and b, respectively.

The spectra and decay kinetics presented on the last graphs show that this sample does not exhibit temperature quenching of Mn^{2+} luminescence up to at least 500 K. Some temperature quenching is observed for Eu^{2+} especially above 350 K.

The decay times of Eu^{2+} are in the sub-microsecond range. Decay kinetics are nonexponential, due to the energy transfer processes between the Eu^{2+} and Mn^{2+} ions. The Mn^{2+} decay times are in the ms range, typical for forbidden type of these optical transitions.

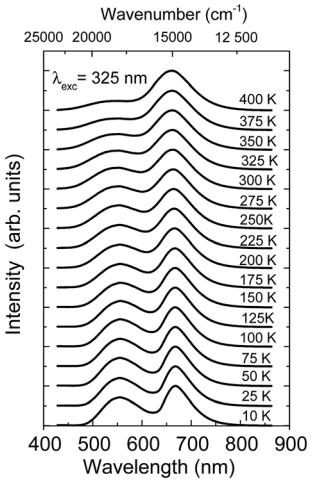

Fig. 3 Temperature dependence luminescence spectra of $NaScSi_2O_6$:Eu(5%),Mn(15%) sample, excited by the 325 nm laser line. The spectra were normalized to the peak of Mn^{2+} luminescence band.

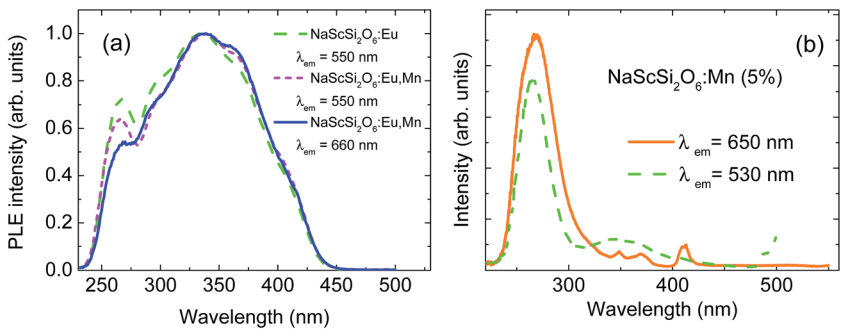

Fig. 2 (a) Normalized room temperature excitation spectra of $ScSi_2O_6$:Eu(5%) and $NaScSi_2O_6$:Eu(5%),Mn(15%) samples monitored at peaks of their luminescence bands. (b) Room temperature excitation spectra of $ScSi_2O_6$:Mn(5%) sample monitored at 530 nm and 650 nm.

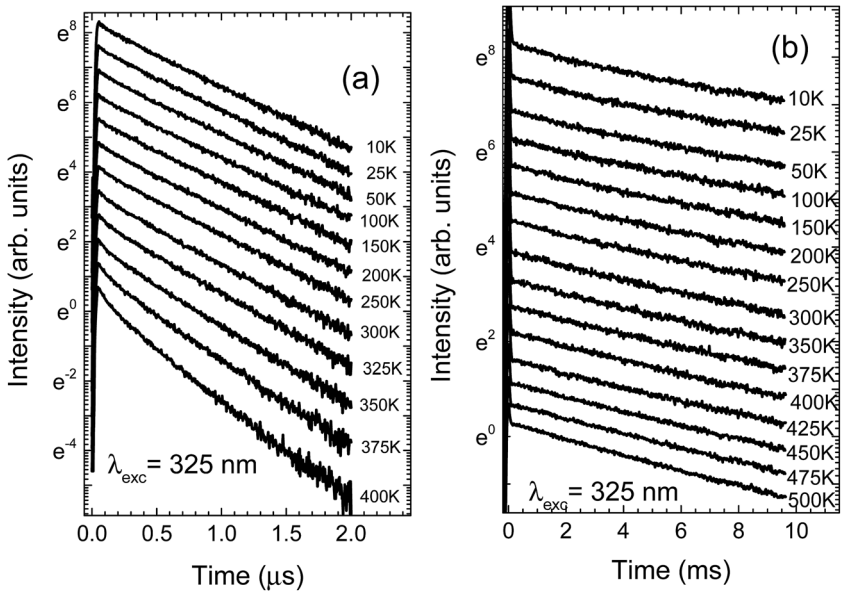

Fig. 4 Temperature dependence of the luminescence decay kinetics of $NaScSi_2O_6$:Eu(5%),Mn(15%) sample, excited by the 325 laser line: (a) decays of Eu^{2+} luminescence; (b) decays of Mn^{2+} luminescence.

The decay kinetics of Eu^{2+} in the sample not doped with Mn^{2+} exhibit much less non-exponential behavior than observed in doubly doped sample. This is another sign of the excitation energy transfer from Eu^{2+} to Mn^{2+} ions. The comparison of the europium ions decay kinetics in samples doped only with Eu^{2+} and doubly doped with Eu^{2+} and Mn^{2+} is presented in Fig. 5.

III.2. High pressure studies

The luminescence spectra of the $NaScSi_2O_6$:Eu(5%),Mn(15%) sample as a function of pressure at room temperature are presented in Fig. 6.

The spectra exhibit shifts of the luminescence peaks towards longer wavelengths, which is approximately linear with pressure in the energy scale. The pressure coefficients for Eu^{2+} are equal to -6.2 ± 0.13 cm^{-1}/kbar and for Mn^{2+} -14.8 ± 0.8 cm^{-1}/kbar, respectively. The shifts reflect the increase of splitting of the 5d level for Eu^{2+} and the decrease of the energy of the first excited level ($^4T_{2g}$) for Mn^{2+} (see appropriate Tanabe–Sugano diagram for d^5 configuration), together with the appropriate Stokes shifts. The positions of the peaks of luminescence of the Eu^{2+} and Mn^{2+} ions as functions of pressure are shown in Fig. 7.

The energy positions of the luminescence peaks during compression and decompression overlap with each other not showing appreciable hysteresis. Eu^{2+} luminescence does not exhibit quenching with pressure in contrast to the luminescence of Mn^{2+}, which intensity decreases with increased pressure in comparison with luminescence of Eu^{2+} and it is completely quenched at pressures above 200 kbar. The origin of that quenching will be discussed later.

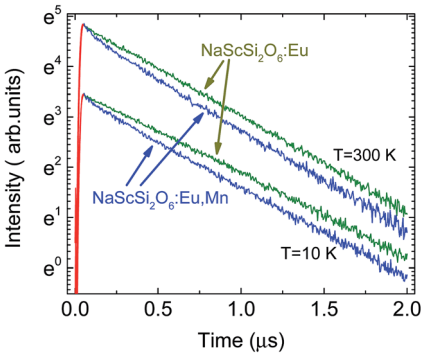

Fig. 5 Comparison of the decay kinetics of Eu^{2+} $NaScSi_2O_6$ in samples doped only with Eu(5%) and doubly doped with Eu (5%) and Mn(15%), excited by the 325 laser line, at 10 K and 300 K.

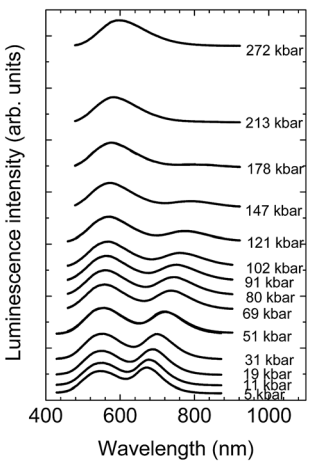

Fig. 6 Luminescence spectra of the $NaScSi_2O_6$:Eu(5%),Mn(15%) sample as a function of pressure at room temperature, excited by 325 nm laser light. The spectra are normalized to the maximum of the Eu^{2+} luminescence. Distances in vertical axis are proportional to the pressure values.

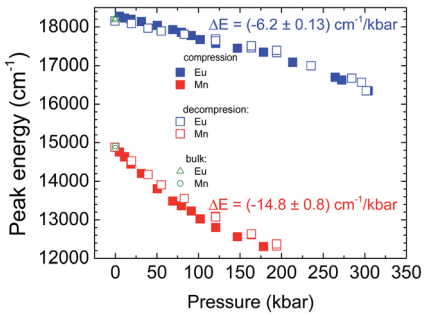

Fig. 7 Positions of the peaks of luminescence of Eu^{2+} and Mn^{2+} ions as functions of pressure for $NaScSi_2O_6$:Eu(5%),Mn(15%) sample. Full points – under compression, open points – under decompression. Open triangle and circle – the positions at ambient pressure (outside of DAC).

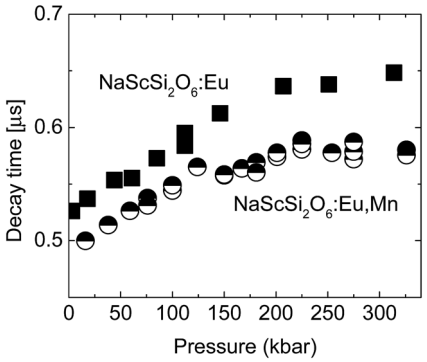

Fig. 9 Pressure dependencies of decay times of longer components of decays for $NaScSi_2O_6$ doped only with Eu(5%) (squares) and doubly doped with Eu(5%) and Mn(15%) (circles).

The examples of the pressure dependence of the decay kinetics of sample doped only with Eu^{2+} and doubly doped with Eu^{2+} and Mn^{2+} are shown in Fig. 8a and b, respectively.

The decay kinetics of the sample doped only with Eu^{2+} are almost single-exponential at low pressures, the nonexponential behavior appears in this sample at high pressures above 100 kbar. In contrast to these results nonexponential decays are observed even at low pressures for sample doubly doped with Eu^{2+} and Mn^{2+}. The decays are faster for this material. For both samples tails of decays (longer components of decays) became exponential. Pressure dependencies of decay times of long components of decays are presented in Fig. 9.

Eu^{2+} decay times of the sample doubly doped are shorter than those for the sample doped only with Eu^{2+}, which is another fingerprint of energy transfer processes occurring in this material. The decay times rise with increasing pressure until the pressure reaches about 200 kbar, and at higher pressures there is no appreciable, consequent increase of decay times.

Decay kinetics of the Mn^{2+} ions present quite different properties. Although with increasing pressure their values also slightly increase, at pressures above 140 kbar a very strong decrease of the decay time is observed, accompanied also by nonexponential decays. The decrease of intensity causes decrease of signal to noise ratio, observed for higher pressures on the decay kinetics. The pressure dependence of the Mn^{2+} decay kinetics is presented in Fig. 10.

Although clinopyroxenes are supposed to be stable with pressure 1, the pressure dependence of the Raman spectra was measured in order to check the crystallographic stability of the measured samples. An example of these results is presented below (Fig. 11).

Similar spectra and pressure relations exhibit both samples doped with Eu^{2+} only and Eu^{2+}/Mn^{2+}. Despite the high level of

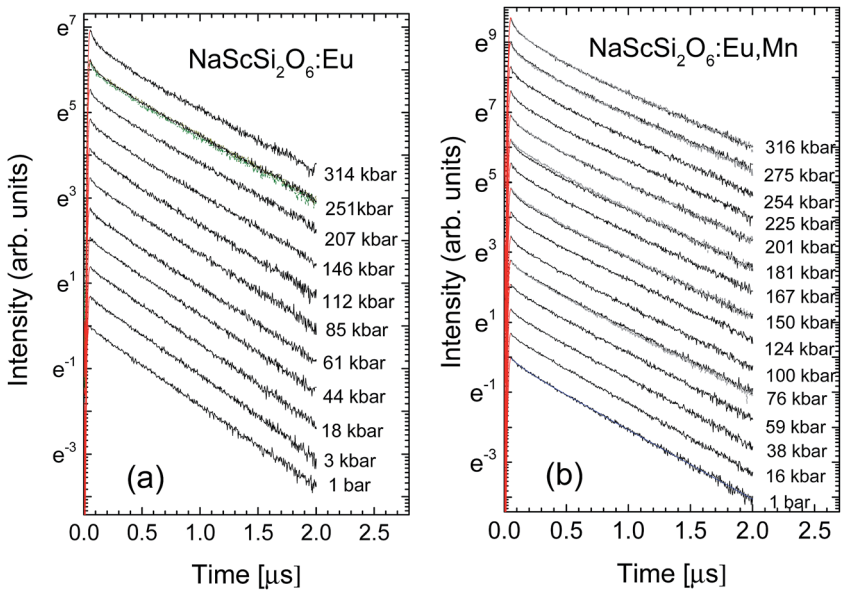

Fig. 8 Pressure dependence of the decay kinetics of Eu^{2+} luminescence at room temperature for: (a) $NaScSi_2O_6$:Eu(5%); (b) $NaScSi_2O_6$:-Eu(5%),Mn(15%) samples.

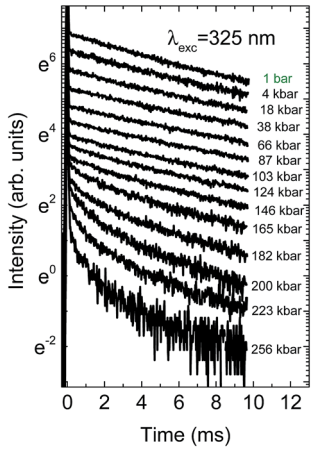

Fig. 10 Pressure dependence of the decay kinetics of Mn^{2+} for $NaScSi_2O_6$:Eu(5%),Mn(15%) sample at room temperature.

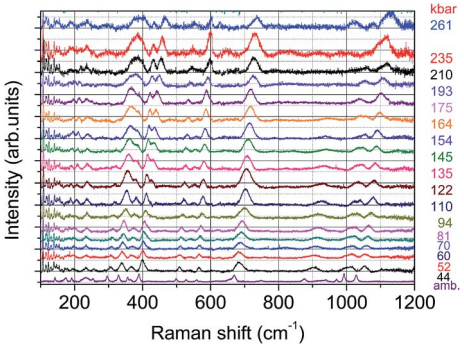

Fig. 11 Raman spectra as a function pressure for $NaScSi_2O_6$:Eu(5%) sample.

doping the spectra show the same peaks at ambient pressure, however with different intensities. The low energy lines observed in the spectra below 150 cm^{-1} are related to argon, which serves as a pressure transmitting medium. Positions of the lines observed in the spectra shift towards higher energies with increasing pressure, however with slightly different pressure coefficients. The lines broaden at higher pressures, which is the most likely associated with certain nonhydrostaticity typical for diamond anvil cells at pressures exceeding 100 kbar. Perhaps the most striking feature observed in the presented spectra is the splitting of the line around 400 cm^{-1} (and above at higher pressures), observed for pressures above 100 kbar. Also some lines change their relative intensities or even disappear at certain pressures. Changes are reversible, *i.e.* after pressure release spectra the same as those before the compression. The more detailed analysis of the Raman spectra will be presented in a separate publication.

IV. Discussion of results

IV.1. Results of high pressure Raman measurements

Similarity of the Raman spectra for the samples doped only with Eu^{2+} and doubly doped with Eu^{2+} and Mn^{2+} is another proof that both types of samples crystallize in the same crystallographic structure. On the other hand it is known that some clinopyroxenes change their structure upon changing content of some constituent ions.[11] The influence of temperature and high pressure on the crystallographic stability of clinopyroxenes was studied in several publications.[12] Although some of them turned out to be stable under influence of these factors, the other showed apparent phase transitions from the $C2/c$ structure to $P2_1/c$ one, and even at higher pressures to the high pressure $C2/c$.[13–17] For these clinopyroxenes $P2_1/c$ is an intermediate phase between both $C2/c$ structures. Some other clinopyroxenes crystallize in the $P2_1/c$ structure at ambient conditions and at higher pressures transform into $C2/c$ phase.[12] One of phase transitions fingerprints is a splitting of some Raman lines. Such a splitting has been observed for example in $LiAlSi_2O_6$ (spodumene) and $LiScSi_2O_6$.[18,19] The both structures are similar and show similar elastic properties, *i.e.* the bulk moduli are not very much different. The phase transition between $C2/c$ and $P2_1/c$ phases is associated with certain reorientation of the structure forming polyhedra and affects the most so called M2 site, *i.e.* the site occupied by Na ions, which may be substituted by Eu^{2+} in case of doping. Therefore both structures do not differ significantly and their changes are reversible upon pressure release.[20] The splitting of the line around 400 cm^{-1} observed at pressure of 122 kbar and above can be also associated with the change of crystallographic structure, most probably similar to those observed in the other clinopyroxenes, *i.e.* from $C2/c$ structure to $P2_1/c$. There is no splitting of the other Raman lines, as it was seen in ref. 18, which is the most probable effect of inhomogeneous broadening associated with high doping level of the examined sample and non-hydrostaticity of the pressure-transmitting medium. The change is reversible, *i.e.* after releasing the pressure the sample exhibit the same spectra like before compression, which testifies that most likely it is a displacive type of the phase transition, similar to observed in the other clinopyroxenes.

Bulk moduli for several clinopyroxenes were measured, however the experimental value for $NaScSi_2O_6$ is not known.[20] Only theoretically predicted value has been given in ref. 20, equal to 109.4 GPa. Also values of pressure derivatives of bulk moduli B'_0 for clinopyroxenes are very often spurious (sometimes even negative).[20] Lack of good knowledge on the nature of phase transitions and poor data quality are often blamed for these discrepancies. Therefore a typical value of $B'_0 = 4$ has been used in further calculations.

IV.2. Pressure dependence of the energy transfer

It has been established in ref. 1 that the dipole–dipole energy mechanism is responsible for the energy transfer between Eu^{2+} and Mn^{2+} ions. The probability P_{ET}^{dd} of such transfer is then described by the formula:[21]

$$P_{ET}^{dd}(R_{DA}) = \frac{1}{\tau_r}\left(\frac{R_0}{R_{DA}}\right)^6 \quad (1)$$

where R_{DA} – is the distance between a donor and an acceptor (in our case distance between the Eu^{2+} and Mn^{2+} ions), τ_r – is the

radiative decay time of the energy donor, and R_0 – is the critical distance, for which the nonradiative energy transfer probability is equal to radiative decay probability of the energy donor. Assuming statistical distribution of energy donors and acceptors the decay kinetics of luminescence are described by the Inokuti–Hirayama model,[22] which for dipole–dipole interaction mechanism is expressed by the formula:

$$I(t) = I_0 \exp\left[-\frac{t}{\tau_r} - \Gamma\left(\frac{1}{2}\right)\frac{C}{C_0}\left(\frac{t}{\tau_r}\right)^{\frac{1}{2}}\right] \quad (2)$$

where C – is the concentration of energy acceptors, C_0 – is the critical concentration, equal to $C_0 = 3/(4\pi R_0{}^3)$, Γ is the gamma function. Subsequent analysis of the decay kinetics and the energy transfer processes will be done according to the procedure proposed in ref. 23.

Since the decay kinetics of the sample doped only with Eu^{2+} exhibit certain nonexponentiality, especially at higher pressure, we propose to treat that nonexponential part as radiative decay. This way the expression given below should yield the value:

$$\ln\left[\frac{I_{Eu,Mn}(t)}{I_{Eu}(t)}\right] = -1.772\frac{C}{C_0}\sqrt{\frac{t}{\tau_r}} = S\sqrt{t} \quad (3)$$

where $I_{Eu,Mn}(t)$ – is the decay kinetics at certain pressure for the doubly doped sample, and $I_{Eu}(t)$ is the decay kinetics of the sample doped only with Eu^{2+} for the same pressure (actually, in the fits the decay kinetic for the sample doped only with Eu^{2+} the decay kinetic for the closest pressure to the pressure at which the sample doubly doped was measured was used). Therefore the plot of the left side of this expression taken from the experimental value as a function of $(t)^{1/2}$ should be a straight line with the slope $S = -1.772\ (C/C_0)/(\tau_r)^{1/2}$. The example of such correlation plots is given in Fig. 12.

Relatively large spread of the data is associated with the important noise of decay kinetics. Its elimination would require considerably longer measurement time. However possibility of fitting the data with the straight line as shown on correlation plots of the type shown in Fig. 12 confirm that the dipole–dipole mechanism of energy transfer is dominating in our material. The pressure dependence of the slopes, S, established from the eqn (3) is shown on Fig. 13a.

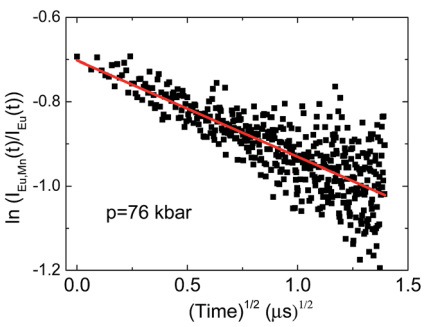

Fig. 12 The correlation plot for $NaScSi_2O_6$:Eu(5%),Mn(5%) sample. The straight line is a fit of eqn (3) to the data.

We assume now that the parameters of the slope, S, are pressure-dependent, *i.e.*:

$$S = -1.772\frac{C(p)}{C_0(p)\sqrt{\tau_r(p)}} \quad (4)$$

through the changes of the of the sample volume and decay time with pressure. The pressure-induced changes of materials volume can be estimated from Murnaghan equation of state:[24]

$$\frac{V}{V_0} = \left[1 + p\left(\frac{B'_0}{B_0}\right)\right]^{-\frac{1}{B'_0}} \quad (5)$$

Assuming that the concentration of energy acceptors (Mn^{2+} ions) is equal to nominal concentration of $C_n = 0.15$ in Sc sites, and the volume of the elementary cell is equal to V_{el} (0 kbar) = 456 Å^3 from ref. 1, it is possible to calculate absolute values of the critical distances R_0^{dd} as function of pressure and also temperature from the following formula:

$$R_0^{dd} = \left(-\frac{3S\sqrt{\tau_r}}{4(\sqrt{\pi})^3 C_n}V_{el}(p)\right)^{\frac{1}{3}} \quad (6)$$

Substituting Murnaghan eqn (5) as a value of $V_{el}(p)$ and using $B_0 = 109.4$ GPa and $B'_0 = 4$ from ref. 20 the changes of critical distance for dipole–dipole mechanism of energy transfer can be calculated as a function of pressure, which is presented in Fig. 13b.

The value of the $(R_0^{dd}(p))^6$ is proportional to the overlap integral between the emission spectrum of the energy donor and absorption spectrum of the energy acceptor (Eu^{2+} and Mn^{2+}, respectively, for our case) through the formula:[21]

$$\left(R_0^{dd}\right)^6 \propto \int_0^\infty \frac{\varepsilon_S(h\nu)\alpha_A(h\nu)}{(h\nu)^4}\mathrm{d}(h\nu) \quad (7)$$

The observed changes are very small, except a strong decrease of the energy transfer efficiency present around pressure at which the phase transition occurs. At higher pressure the efficiency of the energy transfer is restored, and even a small relative increase of this parameter can be detected from Fig. 13b. Large error bars, associated with relatively small accuracy of streak camera and use of DAC does not allow establishing mechanism responsible for this change. Most probably, the overlap integral eqn (7) is changed by pressure application. Nevertheless the increase of the probability of the energy transfer with pressure is not very significant in this material.

Origin of energy transfer suppress at pressure at which the phase transition occurs is not known yet. It might be related to phase-transition induced lattice disorder and reorientations of molecules constituting the crystallographic structure.[25] Perhaps overall quenching of the luminescence occurring around this pressure may be caused by the defect formation during phase transition, which contributes to the decrease of the luminescence efficiency. The increased non-exponentiality of the decay

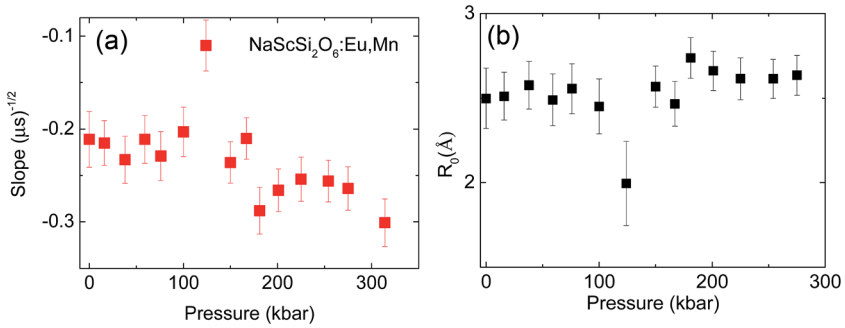

Fig. 13 (a) Pressure dependence of the slopes, S, of the correlation plots for the dipole–dipole energy transfer for $NaScSi_2O_6$:Eu(5%),Mn(15%); (b) pressure dependence of the critical radius of the energy transfer between Eu^2 and Mn^{2+} in this jervisite.

kinetics of the sample singly doped with europium, which occurs around 100–120 kbar is the most probably associated with increasing energy transfer to the defects induced by the phase transition. The exact mechanism of the energy transfer suppress at the phase transition region would require additional studies, which is beyond the scope of this paper.

In contrast to observed small changes of the energy transfer probability with pressure, a slight decrease of the critical distance R_0 is detected. The dependence of the critical distance for dipole–dipole energy transfer, $R_0^{dd}(T)$, on temperature at ambient pressure is shown in Fig. 14.

Observed changes of R_0 with temperature are also small, as well as changing pressure. The obtained values of R_0 seems to be reasonable, taking into account the smallest possible distance between Eu^{2+} and Mn^{2+} ions in clinopyroxene structure, equal to about 3.22 Å at ambient pressure. Relatively larger distance between interacting ions than the critical radius R_0^{dd} prefers longer-distance dipole–dipole interaction in contrast to more effective on shorter distances higher order multipole or exchange interactions. The results will be dependent on total amount of Mn^{2+} ions present in the sample. Our assumption that the total concentration of Mn^{2+} is equal to nominal concentration of substrates seems to be reasonable, since changes in the Mn^{2+} excitation efficiency are at least proportional to the Mn substrate content.[1] However according to eqn (6), exact results on R_0^{dd} is proportional to $C^{-1/3}$, which may change slightly the results if the concentration of Mn^{2+} is different than those calculated from the amount of substrates used for synthesizing these materials.

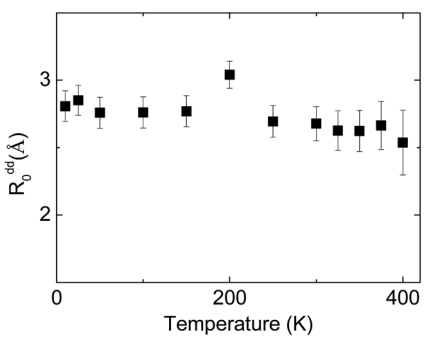

Fig. 14 Temperature dependence of the critical radius of the energy transfer between Eu^{2+} and Mn^{2+} in $NaScSi_2O_6$:Eu(5%),Mn(15%) jervisite at ambient pressure.

IV.3. Pressure-induced quenching of luminescence of Mn^{2+} in $NaScSi_2O_6$:Eu(5%),Mn(15%)

The $NaScSi_2O_6$:Eu(5%),Mn(15%) sample exhibits the Mn^{2+} luminescence with a peak at about 660 nm at ambient pressure, *i.e.* in the red part of the spectrum. This luminescence is associated with the $^4T_{1g} \rightarrow {}^6A_{1g}$ intraconfigurational transitions within $3d^5$ shell of Mn^{2+} ions. Application of high pressures shifts that luminescence band towards infrared with a rate of about 15 cm^{-1}/kbar. The decay kinetics of this luminescence are close to single exponential up to about 150 kbar. Above that pressure the quenching of the luminescence occurs, with apparent participation of nonradiative transitions, which is confirmed by the strongly nonexponential luminescence decay kinetics. The weak luminescence form Mn^{2+} ions is still visible at pressure of about 180 kbar with a peak at about 810 nm. This is the longest wavelength associated with Mn^{2+} luminescence, ever observed, according to our knowledge. The longest wavelength of Mn^{2+} emission ever found before in the other compound is at 725 nm at room temperature.[26] We associated the Mn^{2+} luminescence quenching with the crossing between the $^4T_{1g}$ and $^2T_{2g}$ excited states, which occurs at the pressure of about 200 kbar in this compound. The $^2T_{2g}$ state becomes the first excited state at this pressure. Since it is much stronger coupled to the lattice than the $^4T_{2g}$ state (see the Tanabe–Sugano diagram for the $3d^5$ system, Fig. 15), the excitation energy is nonradiatively transferred to the lattice.

Partial Tanabe–Sugano diagram, presenting appropriate energy levels of Mn^{2+} (d^5) ions is shown on Fig. 14 for the ratio of C/B Racah parameters equal to 4, which is adequate for our system. Previous studies show that the ratio of C/B can be equal between 3.6 up to almost 6.[27–29] The value of Racah parameter B can be estimated from the position of the $^4E_g + {}^4A_{1g}$ levels, which energy is equal to $10B + 5C$. Estimated value of B (for $C/B = 4$) is equal to about 830 cm^{-1}. Although in the system with large Stokes shift it is impossible to see the position of no-phonon lines even the low temperatures, we use approximated values of the energy of pure $^4T_1$ electronic level as the

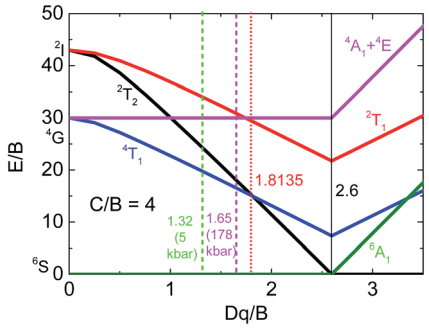

Fig. 15 Partial Tanabe–Sugano diagram for the d^5 configuration in an octahedral crystal field for $C/B = 4$.[30] Vertical lines mark values of D_d/B for: ambient (green) and 178 kbar (magenta) pressures, crossing point between the $^4T_{1g}$ and $^2T_{2g}$ levels (red), and crossing point between high- and low-spin configurations (solid black).

energy at which the luminescence signal is close to the luminescence background at the high energy side of Mn^{2+} emission band. Then the respective positions of the energy levels, (in E/B units), as a function of pressure for 5 kbar and 178 kbar (the highest pressure in which the luminescence of Mn^{2+} is visible) can be calculated. Respective values of crystal field parameter, D_q/B, are established from Tanabe–Sugano diagram. These data are presented in Table 1.

The appropriate positions of electronic levels for 5 kbar and 178 kbar are marked at Tanabe–Sugano diagram (Fig. 15). The value of D_q/B obtained for pressure of 178 kbar is very close to the crossing point between the $^4T_{1g}$ and $^2T_{2g}$ levels, which occurs for $D_q/B = 1.8135$ (for used $C/B = 4$).

The value of D_q parameter should be approximately dependent on the distance, r, between the central ions and ligands as $D_q \sim r^{-5}$. Therefore the ratio $(D_q\ (5\ \text{kbar})/D\ (178\ \text{kbar}))^{1/5}$ equal to 0.956 can be compared with appropriate ratio of the distances obtained from Murnahgan EOS (eqn (5)) (taken as $(V/V_0)^{1/3}$) for an ambient and 178 kbar pressure. This ratio obtained from Murnaghan equation is equal to 0.955, which is in perfect agreement with the value obtained from the crystal field (Tanabe–Sugano diagram) theory. This is also a proof of consistency of our analysis. It should be noticed that larger value of C/B ratio would yield worse agreement between results obtained from the crystal field theory and Murnaghan EOS.

From Tanabe–Sugano diagram the crossing between the $^4T_{2g}$ and $^2T_{2g}$ levels should occur at energy equal to about $E/B \sim 15$, 22 (12 633 cm^{-1} for $B = 830\ cm^{-1}$). Although no emission is expected at the crossing point, taking also into account the Stokes shift between the absorption and emission, the maximum of the luminescence should have occurred at wavelength of about 870 nm. This is longer wavelength than the observed peak of luminescence at highest pressure (around 178 kbar), at which the Mn^{2+} emission is still visible. It is again consisted with presented explanation of the pressure-induced Mn^{2+} luminescence quenching effect. According to our knowledge it is a first observation of such effect in inorganic compounds.

Table 1 Estimated energies of $^4T_1$ electronic level at low and high pressures and respective values of crystal field parameters D_q/B

Pressure (kbar)	Estimated energy of 0-ph line (cm^{-1})	Energy position of $^4T_1$ level in B units ($B = 830\ cm^{-1}$)	Crystal field parameter D_q in B units
5	16 340	19.69	1.32
178	13 643	16.44	1.65

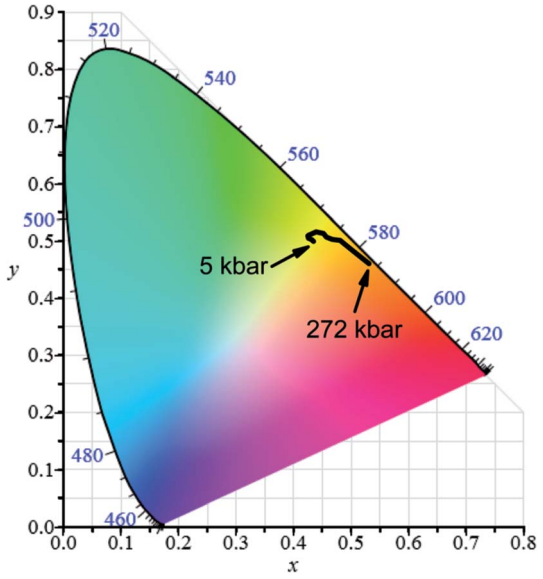

Fig. 16 Chromaticity diagram of $NaScSi_2O_6$:Eu(5%),Mn(15%) jervisite luminescence induced by 325 nm as a function of pressure at room temperature.

IV.4. CIE chromaticity diagram as a function of pressure

The pressure dependence of luminescence color of jervisite phosphor doped with 5% Eu^{2+} and 15% Mn on CIE chromaticity diagram is presented in Fig. 16.

The pressure induced changes of coordinates on CIE diagram of $NaScSi_2O_6$:Eu(5%),Mn(15%) under 325 nm excitation are related to pressure shifts of the luminescence of Eu^{2+} and Mn^{2+}. Actually the pressure shift of Mn^{2+} luminescence towards infrared remove this luminescence component from the visible spectrum at relatively low pressure. This is a reason that at low pressures a slight shift of color towards yellow is observed. At higher pressures a change of color in the direction of red is associated with the pressure-induced shift of the Eu^{2+} luminescence. The quenching of Mn^{2+} luminescence observed at higher pressures does not have important influence on the color of luminescence since the spectrum of Mn^{2+} emission is shifted to the infrared region, not well visible for human eye.

V. Conclusions

The high-pressure measurements of $NaScSi_2O_6$ doped with Eu(5%) and Mn(15%) show that the efficiency of nonradiative energy transfer from Eu^{2+} to Mn^{2+} ions is weakly dependent on pressure. The pressure-induced phase transition, detected by

Raman spectroscopy under pressure, which occurs in this type of clinopyroxenes strongly decrease the efficiency of energy transfer, however only at pressures close to the phase transition. This suggest that decrease of the lattice constant in this type of compounds by so called "chemical pressure" will not significantly increase the efficiency of Mn^{2+} excitation in this type of phosphors. Although the thermal stability of these materials is high, *i.e.* there is practically no thermal quenching of Mn^{2+} up to 500 K. On the other hand high pressure measurements show that the Mn^{2+} luminescence can be quenched by the non-radiative processes associated with the crossing of the $^2T_{2g}$ and $^4T_{1g}$ states of the Mn^{2+} ions. This effect is observed for the first time, according to our knowledge. Also we observed the Mn^{2+} luminescence with a peak at about 810 nm, which is the longest wavelength known for this type of emission.

The excitation spectra of the Mn^{2+} and Eu^{2+} luminescence show that the band gap of examined jervisite at room temperature in *C*2/*c* phase is around 310 nm (4 eV). The pressure-induced change of color of this phosphor is documented by calculations of CIE chromaticity coordinates. They are dominated by pressure changes of Eu^{2+} luminescence spectra.

Acknowledgements

This work was partially supported by the Projects DEC-2012/07/B/ST5/02080 and UMO-2014/13/D/ST3/04032 of the National Science Center of Poland, and Chongqing Overseas Talent Recruitment Program for year 2015. M. G. Brik thanks the supports from the Recruitment Program of High-end Foreign Experts (Grant No. GDW20145200225), the Programme for the Foreign Experts offered by Chongqing University of Posts and Telecommunications, Ministry of Education and Research of Estonia, Project PUT430, and European Regional Development Fund (TK141).

References

1 Z. Xia, Y. Zhang, M. S. Molokeev and V. V. Atuchin, *J. Phys. Chem. C*, 2013, **117**, 20847.
2 S. Y. Wass, *Lithos*, 1979, **12**, 115.
3 https://wwwf.imperial.ac.uk/earthscienceandengineering/rocklibrary/viewminrecord.php?mineral=clinopyroxene.
4 D. Hugh-Jones, T. Sharp, R. Angel and A. Woodland, *Eur. J. Mineral.*, 1996, **8**, 1337.
5 A. B. Woodland, *Geophys. Res. Lett.*, 1998, **25**, 1241.
6 Z. Xia, Y. Y. Zhang, M. S. Molokeev, V. V. Atuchin and Y. Luo, *Sci. Rep.*, 2013, **3**, 3310.
7 Z. Xia, G. Liu, J. We, Z. Mei, M. Balasubramian, M. S. Molokeev, L. Peng, D. J. Miller, Q. Liu and K. R. Poeppelmeier, *J. Am. Chem. Soc.*, 2016, **138**, 1158.
8 A. Kamińska, A. Duzynska, M. Berkowski, S. Trushkin and A. Suchocki, *Phys. Rev. B: Condens. Matter Mater. Phys.*, 2012, **85**, 155111.
9 J. Barzowska, K. Szczodrowski, M. Krośnicki, B. Kukliński and M. Grinberg, *Opt. Mater.*, 2012, **34**, 2095.
10 R. Zhong, X. Meng, M. Li, X. Wang, X. Wen and X. Zhang, *Chem. Phys. Lett.*, 2012, **536**, 55.
11 H. Yang, J. Konzett, D. J. Frost and R. T. Downs, *Am. Mineral.*, 2009, **94**, 942.
12 T. Arlt, M. Kunz, J. Stolz, T. Armbruster and R. J. Angel, *Contrib. Mineral. Petrol.*, 2000, **138**, 35.
13 A. Ullrich, R. Miletich, T. Balic-Zunic, L. Olsen, F. Nestola, M. Wildner and H. Ohashi, *Phys. Chem. Miner.*, 2010, **37**, 25.
14 F. Nestola, T. B. Ballaran, M. Tribaudino and H. Ohashi, *Phys. Chem. Miner.*, 2005, **32**, 222.
15 N. L. Ross and A. Navrotsky, *Am. Mineral.*, 1988, **73**, 1355.
16 P. Comodi, F. Princivalle, M. Tirone and P. F. Zanazzi, *Eur. J. Mineral.*, 1995, **7**, 141.
17 T. Arlt, R. J. Angel, R. Miletich, T. Armbruster and T. Peters, *Am. Mineral.*, 1998, **83**, 1176.
18 M. Tribaudino, L. Mantovani, D. Bersani and P. P. Lottici, *Am. Mineral.*, 2012, **97**, 1339.
19 T. Arlt and R. J. Angel, *Phys. Chem. Miner.*, 2000, **27**, 719.
20 A. C. McCarthy, R. T. Downs and R. M. Thompson, *Am. Mineral.*, 2008, **93**, 198.
21 D. L. Dexter, *J. Chem. Phys.*, 1953, **21**, 836.
22 M. Inokuti and H. Hirayama, *J. Chem. Phys.*, 1965, **43**, 1978.
23 A. Suchocki and J. M. Langer, *Phys. Rev. B: Condens. Matter Mater. Phys.*, 1989, **39**, 7916.
24 F. D. Murnaghan, *Proc. Natl. Acad. Sci. U. S. A.*, 1944, **30**, 244.
25 M. D. Wisser, M. Chea, Y. Lin, D. M. Wu, W. L. Mao, A. Salleo and J. A. Dionne, *Nano Lett.*, 2015, **15**, 1891.
26 M. Muller, S. Fischer and T. Justel, *RSC Adv.*, 2015, **5**, 67979.
27 D. T. Palumbo and J. J. Brown Jr, *J. Electrochem. Soc.*, 1970, **117**, 1184.
28 M.-g. Zhao, G.-r. Bai and H.-c. Jin, *J. Phys. C: Solid State Phys.*, 1982, **15**, 5959.
29 M. C. M. de Lucas, F. Rodiguez and M. Moreno, *J. Phys.: Condens. Matter*, 1993, **5**, 1437.
30 S. Sugano, Y. Tanabe and H. Kamimura, *Multiplets of transition-metal ions in crystals*, Academic Press, 1970.

